Theoretical Demonstration of Hot-Carrier Operation in an Ultrathin Solar Cell

Nicolas Cavassilas, Imam Makhfudz, Anne-Marie Daré, Michel Lannoo, Guillaume Dangoisse, Marc Bescond, Fabienne Michelini

Theoretical demonstration of a hot-carrier operation in ultra-thin solar-cell

Nicolas Cavassilas[1*], Imam Makhfudz[1], Anne-Marie Daré[1], Michel Lannoo[1], Guillaume Dangoisse[2,3], Marc Bescond[1,2] and Fabienne Michelini[1]

[1]*Aix Marseille Université, CNRS, Université de Toulon, IM2NP UMR 7334, 13397, Marseille, France*

[2]*LIMMS-CNRS, IRL 2820, 4-6-1 Komaba, Meguro-ku, Tokyo 153-8505, Japan*

[3]*Ecole Normale Supérieure de Paris, Université PSL, Sorbonne Université, Université de Paris, 75005 Paris, France, 24 rue Lhomond F75005 Paris, France*

*corresponding author: nicolas.cavassilas@im2np.fr

Based on a quantum modeling of the electronic transport, this work shows that ultra-thin solar cells can exhibit an improved open-circuit voltage V_{oc}, without current reduction. This improvement is obtained when an energy-selective contact is considered between the absorber and the reservoir, and is attributed to a hot-carrier effect. While extraction with a non-selective contact does not generate hot-carriers, the use of energy-selective contact induces an increase of carrier temperature up to 130 K and a corresponding V_{oc} enhancement of 41 meV, considering an InGaAs absorber. This enhancement agrees with a simple and general expression formulated in the quantum thermal machine field. Concerning the current, we show that current through an energy-selective contact is of the same order of magnitude as the one obtained without selectivity. This remarkable behavior, which is explained by the hybridization of states in the absorber with the state of the contact, requires a quantum confinement and thus an ultra-thin absorber. Finally, we propose a simple rate-model enabling an intuitive interpretation of the numerical results.

I INTRODUCTION

The hot-carrier solar cell (HCSC) is an elegant concept[1] allowing, in theory, to exceed the limit of Shockley-Queisser (SQ)[2]. The idea, as shown in Fig. 1, is that the carriers remain hot in the absorber where they have been photo-generated by a hot source (the sun). Extracting these carriers through energy-selective contacts (for instance at given energies E_n and E_p for electrons and holes respectively) we can theoretically recover this excess of thermal energy in the form of voltage in the reservoirs. The open-circuit voltage can be formally obtained by a simple expression by assuming two different local thermal equilibriums for the reservoirs and the absorber, and sharp energy filters between these equilibriums. To do so, we consider the entropy balance[3] of the transfer of an electron at energy E_n from the absorber (with a Fermi level μ_{na} and a temperature T_a) to the n-reservoir (with a Fermi level μ_n and at lattice temperature T_L)

$$\Delta S = -\frac{E_n-\mu_{na}}{T_a} + \frac{E_n-\mu_n}{T_L}. \quad (1)$$

The perfect energy selectivity enables an isentropic transfer with ΔS= 0. In this case Eq.(1) shows that both electronic distributions in the absorber and in the n-reservoir must have the same value at the transfer energy E_n.[3] Doing the same analysis for holes at the transfer energy E_p, and summing the two expressions, we finally get[1,4]

$$qV_{oc} = \left(1-\frac{T_L}{T_a}\right)E_{ext} + \Delta\mu_a \frac{T_L}{T_a} \quad (2)$$

with $qV_{oc} = \mu_n - \mu_p$, the open-circuit voltage, $E_{ext} = E_n - E_p$ and $\Delta\mu_a = \mu_{na} - \mu_{pa}$. This expression was derived in the context of quantum thermal machine[3] and extrapolated to the solar cell field[1,4-6]. This equation shows that if $T_a = T_L$ (no hot-carriers), we obtain $qV_{oc} = \Delta\mu_a = \Delta\mu_L$, i.e. the Fermi level splitting when the carriers in the absorber are at the lattice temperature. In this case, which corresponds to a conventional solar cell, V_{oc} is directly related to the rate of the radiative generation and recombination in the absorber and therefore, to its energy bandgap E_g, leading to the SQ limit. On the other hand, if $T_a \gg T_L$ and if electrons and holes are close to equilibrium (for example due to impact ionization)[7], we then have $\Delta\mu_a \approx 0$ and consequently $qV_{oc} \approx E_{ext}$. It is then possible to consider a material for the absorber with a small E_g, to have an significant short circuit current, while considering a contact offering a large E_{ext}, to have a large V_{oc}. We are therefore freed from the trade-off on E_g at the origin of the SQ limit.

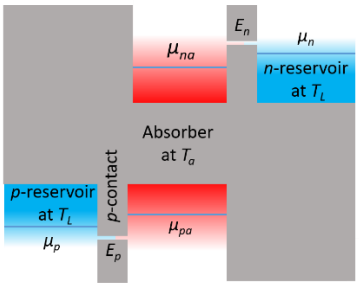

Figure 1. Schematic representation of a hot-carrier solar cell. In the absorber the electron- and hole-distributions are defined by the Fermi levels μ_{na} and μ_{pa} and by the temperature T_a. In both reservoirs the temperature is given by the lattice temperature T_L. The electron-distribution in n-reservoir is defined by μ_n while the hole-distribution in p-reservoir is defined by μ_p. Carriers can transit from the absorber into the reservoirs through contacts at energies E_n and E_p, for electrons and holes, respectively.

In practice, the main difficulty in the development of such solar cells is to obtain a hot-carrier effect, generating a V_{oc} improvement, without degrading the extraction of carriers to preserve the current. Indeed, in isolated system (without contact), hot-carrier distributions have been observed under light illumination in steady-states.[8-10] In such systems the carriers are generated at an average energy $E_{gen} = k_B T_{gen}$ strongly larger than $k_B T_L$. The carriers cool down in a two-step process: *i)* they lose energy by optical-phonon emission, and *ii)* each optical-phonon splits into two acoustic phonons. Assuming a reservoir of acoustic-phonons at the lattice temperature T_L, generated carriers thermalize at an energy T_c located between T_{gen} and T_L. If the cooling rate is larger than the generation rate, T_c is close to T_L, while if the generation rate is larger than the cooling rate, T_c is close to T_{gen}.[11] The goal is thus to increase the generation rate with a large power illumination, and to reduce the cooling rate. In case where the cooling is limited by the optical-acoustic rate, hot-carriers emit optical phonons which are preferentially reabsorbed by the carriers rather than split into two acoustic phonons. This behavior seems to be at the origin of hot-carrier in bulk[10,11] but could also explains observations made in quantum wells.[12] Moreover, in quantum well, due to more restrictive selection rules, the carrier-optical phonon rate can also be reduced. In all cases, these strategies to reduce the cooling rate are called the phonon bottleneck.

In opposition to an isolated system, we can consider a system in which the absorber is perfectly connected to a reservoir. This means that electronic states of the absorber are totally delocalized in the reservoir and vice versa. A priori, the most favorable case is when a generated hot-carrier can ballistically reach the reservoir, before experiencing an optical phonon emission. However, once in the reservoir, such an electron cools down. Moreover, at V_{oc}, the ballistic carrier is replaced by a cold carrier coming from the reservoir. Hence, the electronic distribution in the absorber is almost equal to that of the reservoir and hot-carrier effect cannot be observed.

A practical HCSC has to maintain the carriers hot by isolating the absorber from the cold reservoir, and on the other hand, it has to enable an efficient extraction of carriers. Those two requirements might be seen as contradictory, but quantum mechanism can break this paradox with a resonant tunneling behavior.[13,14] As we have already investigated,[15] if the absorber is a quantum well, one of the confined states hybridizes with the resonant state in the energy-selective contact. It results an efficient extraction of the photo-generated carriers than can be assisted by phonon scattering. This hybridization is equivalent to delocalize the absorber states into the reservoir, but only at a chosen energy-window. For the other energies, and particularly when the electronic distribution in the reservoir is larger than that in the absorber (close to the band edge), the isolation has to be severely preserved.

In this theoretical article, we confirm that the use of an ultra-thin absorber enables to implement the hot electron strategy. In such a structure, considering an electron selective contact, consisting of a double barrier and a quantum dot (QD) or a quantum well (QW), our numerical calculations show that V_{oc} varies with the extraction energy E_n. Since such variations of V_{oc} are consistent with equation (2), they are attributed to the hot-carrier behavior. Moreover, we confirm that the absorption current is preserved by the energy-selective contact. Advances in the fabrication of ultra-thin solar cells, based both on the control of contacts and on the photonic environment, could therefore result in HCSC developpment.[16]

II. METHODOLOGY

To carry out this study, we model ultra-thin cells with the non-equilibrium Green's functions (NEGF) formalism in a self-consistent framework with the Poisson equation. This physical model, which includes the effects of interactions in a picture of quantum transport, is widely used in the field of semiconductor quantum devices.[17-19] It indeed enables to accurately consider behaviors such as quantum confinement, tunneling, electron-phonon and electron-photon scatterings and to model the effects of the semi-infinite reservoirs.

Here, we consider a multi-unidimensional model,[17] meaning that we consider a unidimensional potential along the transport direction, and an invariant potential in transverse plane. In this plane, the dispersions of electron and hole are reproduced by a discretization of the transverse wave-vector k_t. For these dispersions we assume the effective mass approximation which is also considered in the transport direction. For QD, we do not consider such a transverse dispersion, equivalent to a null transverse kinetic energy. In the present model, this is the only difference between QD and QW. Consequently, the energy position of the confined state is controlled in both cases by the distance between the two confining barriers, while for three-dimensional QD it should be controlled by its shape. This approach is suitable for QD offering an oblate spheroid shape. It also enables to treat any other cases considering that the distance between the two confining barriers is effective. At the boundaries of the devices, in the transport direction, we assume semi-infinite reservoirs meaning that the potential in the reservoir is invariant on semi-infinite length and that electrons follow a thermal distribution at 300 K inside these reservoirs.

In the present study, we consider electron-photon, electron-optical phonon and electron-acoustic phonon scatterings. For scattering with photons, in order to simulate conditions close to the experimental ones,[20] we suppose that the cells are illuminated by a 954 nm laser with a power of 1 kW.cm^{-2} (power equivalent to 10^4 suns). On the other hand, the cells can emit photons at any energy, such an emission being due to the interband radiative recombination. Note that we assume the radiative approximation, i.e. non-radiative recombinations are neglected.

For scattering with phonons, we consider that both optical and acoustic phonons remain at T_L =300 K. Indeed, we only calculate the Green functions of the electrons while phonons are considered at thermodynamical equilibrium. We are aware that this approximation is a limitation of our model. But, this limitation reduces the observed hot-carrier effect. Thus, our model cannot overestimate the conclusions of the present work.

Another substantial approximation is that we do not consider the electron-electron interaction in the active region. This scattering does not diffuse energy and therefore does not participate to the cooling. But it favors the transition from an out-of-equilibrium distribution to a Fermi distribution. This approximation explains why the distribution obtained in the present work are not well described by a Fermi function. Note that this interaction is intrinsically taken into account in the reservoir in which Fermi distributions at room temperature are imposed.

The model we employ is fully described in Ref. [17], but we summarize below the principal lines of the NEGF framework, using matrix representation and considering that all constants equal 1 (the Planck constant $\hbar$, the elementary charge q, the transverse surface of the cell, the position mesh along the transport direction and π). For each transverse wave-vector k_t, we define a Hamiltonian matrix $H_{c,v}$ for

the conduction band (CB) and the valence band (VB). Diagonal matrices α represent the potential on each space-point along the transport direction, while the off-diagonal β matrices represent the hopping between two successive space-points. The potential is self-consistently calculated with the Poisson equation. The retarded component of the Green's function (function of E, the electronic energy) is determined from this Hamiltonian matrix following

$$G_{c,v}^{r} = \left[E - H_{c,v} - \Sigma^{r}\right]^{-1} \quad (3)$$

where Σ^{r} is the sum of the self-energies describing the influence of reservoirs and the different scatterings taken into account. The imaginary part of the diagonal terms of $G_{c,v}^{r}$ provides the local density-of-states (LDOS) defined versus both position and energy. Then, the lesser and greater components of the Green's function are calculated from the retarded Green function

$$G_{c,v}^{\lessgtr} = G_{c,v}^{r}\Sigma_{c,v}^{\lessgtr}G_{c,v}^{r\dagger} \quad (4)$$

where $\Sigma_{c,v}^{\lessgtr}$ are the lesser and greater self-energies which will be defined in the following. The imaginary parts of the diagonal terms of $G^{<}(G^{>})$ provide the electron (hole) density. The off-diagonal terms are related to the spectral current between two successive space-points $J_{c,v} = \beta_{c,v}\mathrm{G}_{c,v}^{<} - \beta_{c,v}^{\dagger}\mathrm{G}_{c,v}^{>}$ giving the total current $J = J_v + J_c$. Such a current is defined in position and in energy and can then be shown by a two-dimensional plot (Figs. 2a, b and c in the following).

The lesser and greater self-energies are defined as the sum of the self-energies relative to the influence of electron-photon interaction (*optical*), to the electron-phonon scattering (*scattering*) and to the boundaries condition with the semi-infinite reservoirs (*reservoirs*)

$$\Sigma_{c,v}^{\lessgtr} = \Sigma_{c,v(optical)}^{\lessgtr} + \Sigma_{c,v(scattering)}^{\lessgtr} + \Sigma_{c,v(reservoirs)}^{\lessgtr}. \quad (5)$$

Here we focus only on the optical component which is given by $\Sigma_{c,v(optical)}^{>,<} = M_{op}^{2}\left(N_{op}+1\right)G_{v,c}^{>,<}$ and $\Sigma_{c,v(optical)}^{<,>} = M_{op}^{2}N_{op}G_{v,c}^{<,>}$ with M_{op} the optical matrix element and the number of photons N_{op} (given by the Bose distribution). Once we have the total $\Sigma_{c,v}^{\lessgtr}$, we can evaluate the retarded self-energy using $\Sigma_{c,v}^{r} = (\Sigma_{c,v}^{>} - \Sigma_{c,v}^{<})/2$, which is needed to calculate the retarded Green function with Eq.(3). To assess the functioning of the cell, we will also rely on the electrons flux across the bandgap due to the processes of photon absorption and emission

$$J_{abs} = \Sigma_{c(optical)}^{<}G_{c}^{>} = M_{op}^{2}N_{op}G_{v}^{<}G_{c}^{>}, \quad (6)$$

$$J_{rec} = \Sigma_{v(optical)}^{<}G_{v}^{>} = M_{op}^{2}\left(N_{op}+1\right)G_{c}^{<}G_{v}^{>}. \quad (7)$$

J_{abs} is proportional to the hole density in CB ($G_c^{>}$) times the electron density is VB ($G_v^{<}$), while J_{rec} is proportional to the electron density in CB ($G_c^{<}$) times the hole density in VB ($G_v^{>}$). Finally, note that if electrons (holes) can only be extracted in the n(p)-contact, we have the total current $J = J_{abs} - J_{rec}$. This condition is respected in the devices investigated in the present work.

Since the diagonal elements of $G_{c,v}^{r}$ give the LDOS and the diagonal elements of $G_{c,v}^{\lessgtr}$ give the electron and hole densities, we can calculate the distribution functions of carriers in CB and VB. The LDOS also enables to determine the extraction energy E_n, since the state localized between the two barriers is visible on a two-dimensional plot of the LDOS versus position and energy (Fig. 3 in the following). All

these quantities are obtained for a bias applied between the two reservoirs. To obtain the open-circuit voltage, we interpolate the bias giving $J = J_{abs} - J_{rec} = 0$ (linear and exponential interpolations versus the bias for J_{abs} and J_{rec}, respectively).

III. RESULTS

Figure 2 represents the band diagrams and the current spectra obtained for three different contacts at a voltage of 0.7 V (μ_p=0 eV and μ_n=0.7 eV). This contact is either a simple tunnel barrier (Fig. 2a), thus non-selective, or a QD between two tunnel barriers (Fig. 2b and c), thus selective. In Figs. 2b and c the size of the QD varies, thus modifying the extraction energy E_n (0.94 eV and 1.02 eV respectively). In all three cases, we consider an InGaAs absorber, 12 nm thick, with an InP p-reservoir and an InGaP wetting layer. The n-reservoir is also made of InP but is separated from the absorber by the contact. The two confining barriers of the n-contacts are in AlGaAsSb.

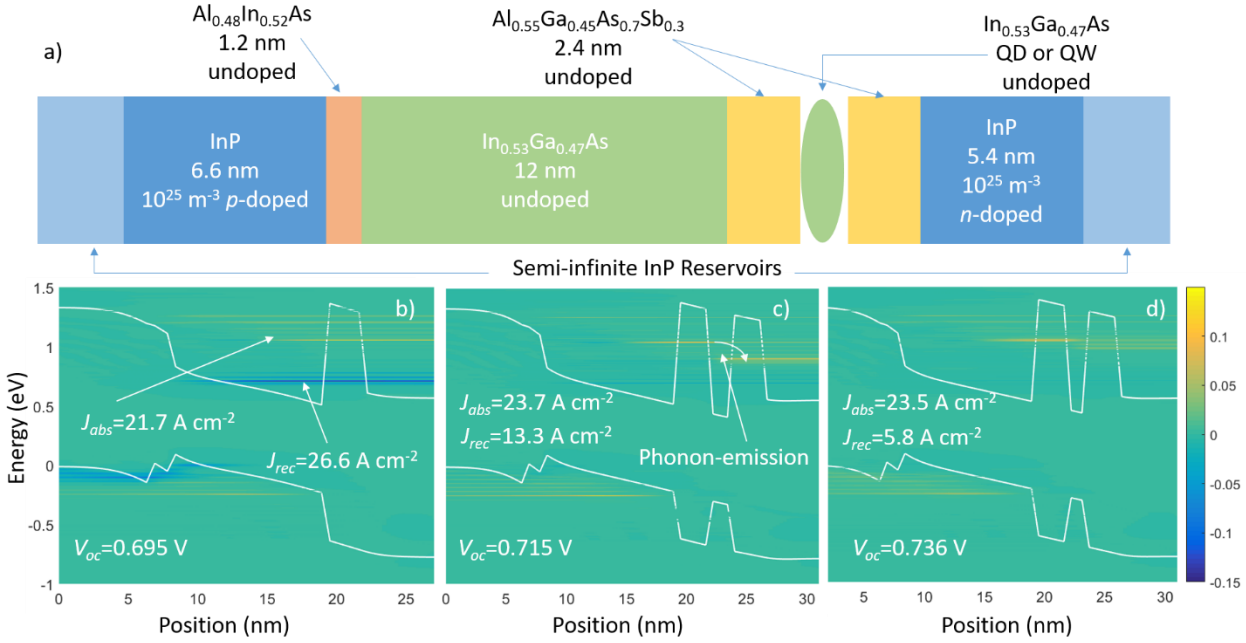

Figure 2. a) Schematic representation of the considered cell. Band diagrams and two-dimensional plot of the current spectra J (in arbitrary unit) of the ultrathin InGaAs solar cell (12 nm), b) with a non-selective contact, c) with a selective contact with E_n=0.94 eV (1.5 nm thick QD) and, d) with E_n=1.02 eV (1.2 nm thick QD). In all cases the reservoirs are in InP and contacts between the absorber and the n-reservoir are made with barrier of AlGaAsSb. For the selective contact, we assume a QD between the two barriers. The Fermi level in p-reservoir is μ_p=0 eV, while in n-reservoir μ_n=0.7 eV. For the three cells we give J_{abs} and J_{rec} calculated at bias equals to 0.7V. Note that, as suggested by the arrows in panel b), J_{abs} corresponds to the positive component of J (in yellow), while J_{rec} corresponds to the negative one (in blue). We also give the open-circuit voltage which is the interpolated bias giving $J_{abs} = J_{rec}$.

As shown in Fig. 2, the absorption currents[21] J_{abs} are 21.7, 23.7 and 23.5 A cm^{-2}, for the cell without selectivity and for E_n=0.94 eV and 1.02 eV, respectively. As shown in Eq.(6), J_{abs} is proportional to the hole density in CB, $G_c^>$, which is related to the LDOS and to the occupancy. The change of LDOS in the absorber with the different n-contacts (simple or double-barrier) is negligible. Another way to explain the variation of J_{abs} is the extraction of carriers by the n-contact. In case of a reduced extraction, the electron density increases in absorber. This corresponds to a decrease of hole density in CB and thus to a decrease of J_{abs}. We thus conclude that extraction is more efficient when a selective contact is

considered. To explain this result, we represent in Fig. 3 the density-of-states in the cell with E_n=1.02 eV. The third state of the absorber hybridizes with the state in the QD.[15] An electron on this state is thus delocalized in the contact and then in the reservoir. Moreover, thanks to the assistance of optical phonon-emission, this extraction is even more efficient. This phonon-assisted extraction can be seen on the current-spectra represented in Fig. 2, where in case of non-selective contact the current absorption (the positive one) is ballistic, while phonons contribute in the cases of selective contacts. Such a hybridization appears only when electrons are confined in absorber. In case of a bulk absorber, as considered theoretically[22] and experimentally,[23] a consequent reduction in current is observed with selective contact. Concerning the recombination current (the negative contribution on current spectra in Fig. 2), at a given bias, the amplitude is reduced with the selective contacts. This confirms that the isolation, at band-edge, is much more efficient with the double-barrier.

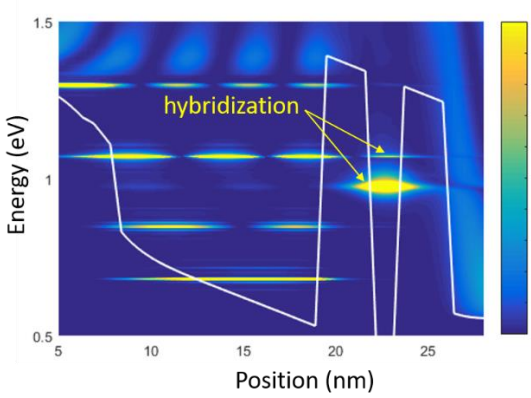

Figure 3. Band diagram and two-dimensional plot of the local density of states (LDOS) (in arbitrary unit), in the absorber and contact, for one transverse mode k_t, calculated in the device presented Fig. 2c with E_n=1.02 eV. Between the two barriers, in the QD, the local density of states shows 2 states. The higher one is due to the hybridization with the third state in the absorber. The consequence of this hybridization is that electrons on this third state on the absorber is delocalized in the contact.

Concerning the open-circuit voltage, V_{oc_num}, we obtain 0.695 V (non-selective), 0.715 V (E_n = 0.94 eV) and 0.736 V (E_n = 1.02 eV). We see that the non-selective contact cell offers the weakest V_{oc_num} and that V_{oc_num} increases with the extraction energy E_n. We then calculate the electronic distribution in the absorber and in the n-reservoir following the Kubo-Martin-Schwinger relation[24]. These distributions are plotted as a function of the energy on Fig. 4 for the three devices of Fig. 2. As expected, the distribution in the three n-reservoirs is exactly equal to the Fermi function with μ_n=0.7 eV and T=300 K. The distribution in the absorber, for the three cases, exhibits a ballistic component at large energy corresponding to the generated electrons before they emit phonons. These ballistic electrons are a-thermal and represent a negligible proportion of the total electronic density. The difference between the three devices concerns electrons having experienced scattering and is observable at lower energy (denoted thermal or pseudo-thermal). When considering a simple tunnel barrier (Fig. 4a), the distribution in the absorber is almost equal to the contact distribution, i.e. no hot-carrier effect is observed. With a selective contact (Fig. 4b and c), the distributions in the absorber are unusual and correspond to out-of-equilibrium electrons. We first see that they depict peaks. Observation of the distribution for each transverse wave-vector k_t shows that these peaks are related to the optical phonon, since they are spaced apart by the energy of the optical phonon. Independently of these peaks, we propose to fit (insets of Fig. 4) these two distributions by a Fermi function. We obtain μ_{na}=0.62 eV and T_a=430 K for E_n=0.94 eV and μ_{na}=0.6 eV and T_a=430 K for E_n=1.02 eV. Even though we cannot

rigorously consider an equilibrium and thus a temperature, this result shows that such selective contacts isolate well enough the absorber, from the reservoirs, to allow the electrons in the absorber to maintain a hot pseudo-thermal distribution. This result also shows that a hot equilibrium can be obtained although optical phonons are at lattice temperature. Considering hot phonons should increase the electronic temperature.

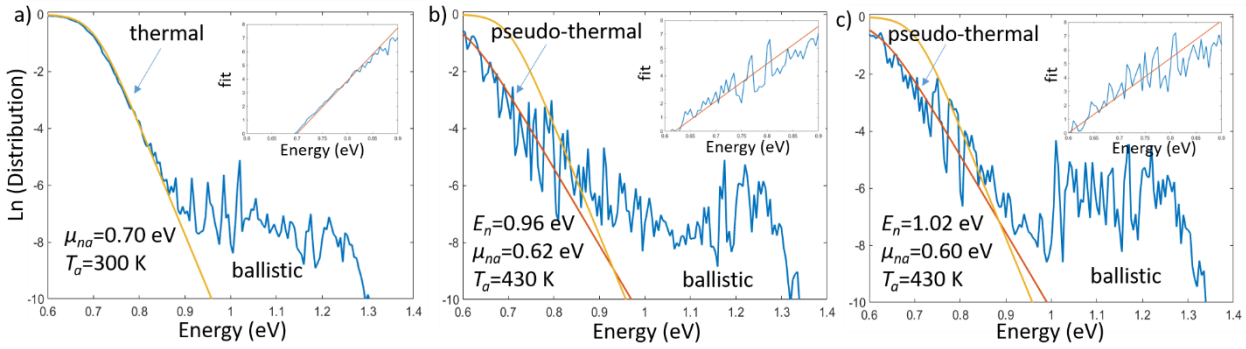

Figure 4. Natural logarithm of the electronic distribution, versus energy, of cells presented in Fig. 2, in absorber (blue line) and in n-reservoir (yellow line). We also represent, in red, the fit of the distribution in the absorber obtained with a Fermi function. To obtain this fit we represent fit=ln(1/distribution-1) versus the energy. The corresponding curves are in inset.

To confirm the link between V_{oc} and this hot pseudo-equilibrium distribution, we modify equation (2) in order to consider the holes are at T_L. Indeed, in absorber we obtain holes at room temperature, for any considered cell, with the same Fermi level as in the left reservoir $\mu_p = 0$ (not shown). This absence of hot holes was expected since we do not consider selective contact. We then obtain this new equation for V_{oc_an} (*an* for analytical):

$$V_{oc\_an} = \left(1 - \frac{T_L}{T_a}\right) E_n + \mu_{na} \frac{T_L}{T_a} - \mu_p. \qquad (8)$$

By applying this expression to the two cells with E_n=0.94 eV and 1.02 eV, and by considering the corresponding μ_{na} and T_a, we find respectively V_{oc_an}=0.717 V and 0.727 V (*versus* V_{oc_num}= 0.715 V and 0.736 V obtained by simulations). These values should be compared to 0.695 V, the numerical V_{oc} obtained without hot-carriers. The agreement between the numerical and the analytical values confirms that the improvement of V_{oc_num} with the selectivity of contact is due to a hot-carriers effect.

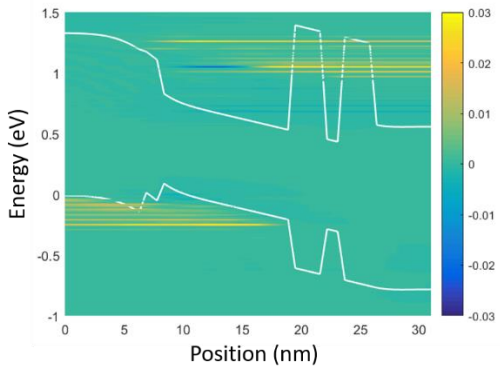

Fig. 5. Band diagrams and two-dimensional plot of the current spectra J (in arbitrary unit) of the ultrathin InGaAs solar cell (12 nm), with a semi-selective contact (QW) with $E_n = 1.02$ eV (with a 1.2 nm thick InGaAs QW).

We also conducted calculations for a semi-selective contact considering a QW rather than a QD. In this case, with E_n=1.02 eV, we obtain numerically J_{abs}=20.3 A cm^{-2}, V_{oc_num}=0.728 V, μ_{na}=0.62 eV and T_a=400 K, which gives V_{oc_an}=0.720 V. Even in the case with QW, the numerical and analytical values are in good agreement. Compared to the case with the QD contact having the same E_n, all the criteria show a less efficient solar cell. Particularly, the current spectra represented Fig. 5 shows that, likewise to the case with a simple barrier, the current is mainly ballistic. This means that the hybridization observed with the QD contact does not assist the extraction, explaining the smaller J_{abs} (20.3 versus 23.5 A cm^{-2}). However, while a selective contact seems necessary for optimal operation, with the semi-selectivity the effect of hot-carriers is significant. Since it is much easier to fabricate a semi-selective contact, this result is very encouraging for a future experimental demonstration of HCSC.

IV. DISCUSSION

In this section we propose a discussion based on a simple rate-model which is schematically represented Fig. 5. We consider three electronic states numbered 1, 2 and 3 of energies $E_1 < E_2 < E_3$ and with the distributions f_1, f_2 and f_3. By emitting or absorbing a phonon, electrons can change of state with the respective rates $\sigma_{em}$and σ_{ab} given by

$$\sigma_{ab} = M^2 N \tag{9}$$

$$\sigma_{em} = M^2(1+N) \tag{10}$$

with M the electron-phonon scattering matrix element and $N = 1/(exp(\hbar\omega/k_B T_L) - 1)$ the number of optical phonons of energy $\hbar\omega$ which is given by the Bose distribution at T_L=300 K. Assuming $n > m$, the corresponding electrons flux between the states n and m is given by $\sigma_{em} f_n(1-f_m) - \sigma_{ab} f_m(1-f_n)$. We also consider a radiative generation flux G, corresponding to the laser excitation, injected on the state 3. This involves a recombination flux from each state n given by Rf_n, with $G = R(f_1 + f_2 + f_3)$ at V_{oc} and with R the interband recombination coupling (spontaneous emission) given by

$$R = M_{op}^2(1-f_v) \tag{11}$$

with M_{op} the interband optical matrix element and f_v the electronic distribution in the valence band. In stationary regime, the net flux on any state equals zero and we can calculate f_1 and f_3 versus f_2 and the other parameters

$$f_1 = \frac{\sigma_{em} f_2}{\sigma_{ab} + f_2(\sigma_{em} - \sigma_{ab}) + R} \tag{12}$$

$$f_3 = \frac{R(f_1+f_2) + \sigma_{ab} f_2}{\sigma_{em} - f_2(\sigma_{em} - \sigma_{ab})}. \tag{13}$$

In the following, we will compare the reservoir with doping but without illumination, and the absorber under illumination. We impose the same value of f_2 for the two cases. This will allow us to consider an isentropic transfer through a selective contact at E_2. In dark, this value of f_2 is related to the doping, while under illumination and for a given R, it can be experimentally obtained by tuning the incident photon flux.

Fig. 6a shows result obtained for $f_2 = 10^{-4}$, in the reservoir. In this case the resulting distribution f_n, which does not depend on M, exhibits the shape of a Boltzmann distribution (exponential versus energy). Considering that energy between the states equals the phonon energy, this Boltzmann

distribution is at 300 K. This simple rate-model can then describe electrons at the equilibrium with the phonons.

We present in Fig. 6b the result in absorber under illumination, with $R = 0.2M^2$. As suggested in the two equations (12) and (13), the distribution at high energy E_3 increases while it is reduced at low energy E_1. But, we can no longer define a temperature because the distribution does not have an exponential shape. However, increasing the high energy distribution while reducing the low energy distribution is equivalent to heating the electrons. We thus obtain a pseudo hot equilibrium regime by simply generating electrons at E_3, a higher energy than the average energy of the corresponding recombination $(E_1 f_1 + E_2 f_2 + E_3 f_3)/(f_1 + f_2 + f_3)$. This result is in agreement with the numerical calculation presented in this work and shows that, even with cold phonons, it is possible to obtain a pseudo hot equilibrium.

Concerning the evolution with the different parameters, for a given R, we verified that hot-carrier effect increases with G. This is not surprising since experimentally a powerful illumination is needed to observe hot-carrier effect. We also verified that for a given G, this hot-carrier effect increases with R. This last result, considering Eq. 11, suggests that an empty VB (with a large hole density) and a strong optical coupling are both beneficial for the hot-carrier effect.

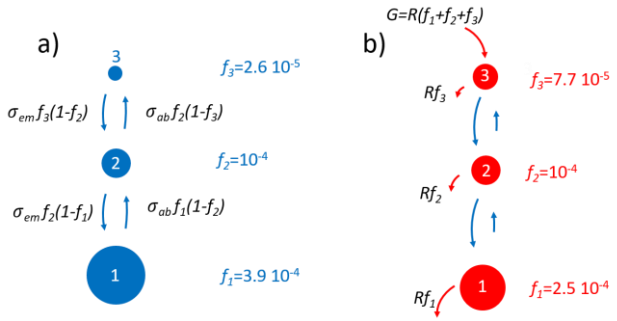

Fig. 6. Schematic representation of the rate-model and of the resulting distributions a) at the thermodynamical equilibrium in the reservoir, and b) with a radiative generation on the top state 3 with R=0.5M in the absorber. For each state, the disk surface is proportional to the distribution. For both calculations f_2 is imposed to 10^{-4}, the number of phonons N is unchanged (phonons stay cool) and the energies of the states are given by $E_n = \hbar\omega(n-1)$ with $\hbar\omega = 35\ meV$ the phonon energy and n the index of the state. Blue disks are chosen when distribution is cool while red disks represent a hot distribution.

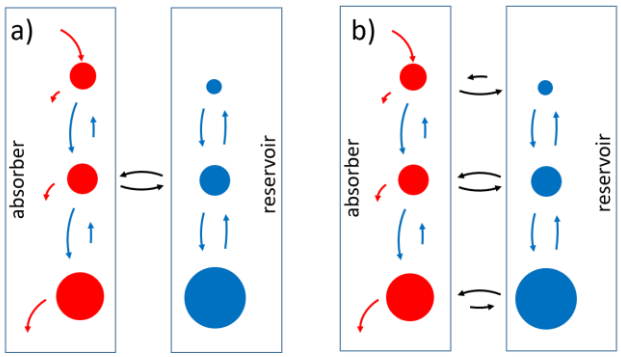

Fig. 7. Schematic representation of a hot absorber connected to a cold reservoir at V_{oc} with a) a selective contact allowing an isentropic extraction, and b) with a non-selective contact. While the isentropic extraction does not modify the electronic distribution in the absorber, the non-selective contact should cool the electrons in the absorber. Blue disks are chosen when distribution is cool while red disks represent a hot distribution.

We now consider that this pseudo hot distribution is an absorber connected to the cold distribution, defined as the reservoir. Fig. 7a shows when an isentropic extraction is considered, meaning with a selective contact whose energy E_n is located such that the hot and cold distributions are equal. In this case, at V_{oc}, the hot distribution is not disturbed by the contact. On the other hand, Fig. 7b shows the case where a non-selective contact is considered. With such a contact the net electron flux is oriented from the reservoir into the absorber at low energy and in the inverse direction at high energy. This will thus reduce the distribution of the absorber at high energy while it will increase it at low energy. In other words, such a contact will cool the electrons in the absorber. These results are also in agreement with the numerical calculations conducted in the present work.

IV. CONCLUSION

This article shows that, under powerful laser illumination, an ultra-thin solar cell associated with energy-selective contact exhibits a larger V_{oc} without current degradation. In spite of the selective contact our quantum model shows that the current is not degraded thanks to a hybridization behavior. The improvement of V_{oc} is related to a hot-carrier effect which can be explained by a simple rate model. Such an effect increases with the selectivity but still exists in realistic design such as contact made with QW. This result should be more visible by considering hot phonons and should not be reduced by the carrier-carrier scattering. This behavior could be experimentally demonstrated by the V_{oc} comparison of ultra-thin solar cells with a simple barrier and with a double-barrier as contact. If the current is not degraded by the selectivity, as shown by our results, such a measurement would be a demonstration of a hot-carrier solar cell operation. However, it should be note that the hot carriers effect exists only if the incident light power is sufficient (10^4 suns here). This implies an important electron current density which can cause problems related to the practical extraction of the current.[25]

Moreover, an interesting result shown in this article is that, assuming a sophisticated numerical model including realistic materials under illumination, we confirm the validity of the very general expression of V_{oc} (Eq.(2)), in both QD and QW geometries.

In the future, a study concerning the design of the contact would be interesting to better understand the impact of hybridization and selectivity in cell under a concentrated solar spectrum. It would be also interesting to consider non-radiative recombination processes which should, as suggested in the present work, impact the hot-carrier effect.

ACKNOWLEDGEMENT

The authors thank ICEMAN (ANR-19-CE05-000) for financial support.

REFERENCES

[1]R. T. Ross and A. J. Nozik, “Efficiency of hot-carrier solar energy converters,” J. Appl. Phys. **53**(5), 3813–3818 (1982).

[2]W. Shockley and H. J. Queisser, “Detailed balance limit of efficiency of p-n junction solar cells,” J. Appl. Phys. **32**(3), 510–519 (1961).

[3]T. E. Humphrey, R. Newbury, R. P. Taylor, and H. Linke, "Reversible Quantum Brownian Heat Engines for Electrons," Phys. Rev. Lett. **89**(11), 116801-116805 (2002).

[4]A. Pusch, M. Dubajic, M. P. Nielsen, G. J. Conibeer, S. P. Bremner, and N. J. Ekins-Daukes, "Optoelectronic reciprocity in hot carrier solar cells with ideal energy selective contacts," Prog. Photovolt. Res. Appl. **29**, 433-444 (2021).

[5]S. C. Limpert and S. P. Bremmer, "Hot carrier extraction using energy selective contacts and its impact on the limiting efficiency of a hot carrier solar cell", App. Phys. Lett. **107**, 073902 (2015).

[6]S. C. Limpert, S. Bremmer and H. Linke, "Reversible electron-hole separation in a hot carrier solar cell", New J. Phys. **17**, 095004 (2015).

[7]P. Würfel, "Solar energy conversion with hot impact ionization," Solar Energy Materials and Solar Cells **46**, 43-52 (1997).

[8]D.-T. Nguyen, L. Lombez, F. Gibelli, S. Boyer-Richard, A. Le Corre, O. Durand, J.-F. Guillemoles, "Quantitative experimental assessment of hot carrier-enhanced solar cells at room temperature," Nature Energy **3**(3), 236-242 (2018).

[9]L.C. Hirst, H. Fujii, Y. Wang, M. Sugiyama, N.J. Ekins-Daukes, "Hot carriers in quantum wells for photovoltaic efficiency enhancement," IEEE Journal of Photovoltaics **4**(1), 244-252 (2013).

[10]M. Giteau, E. de Moustier, D. Suchet, H. Esmaielpour, H. Sodabanlu, K. Watanabe, S. Collin, J.-F. Guillemoles, Y. Okad, "Identification of surface and volume hot-carrier thermalization mechanisms in ultrathin GaAs layers," Journal of Applied Physics **128**(19), 193102 (2020).

[11]C.-Y. Tsai, "Theoretical model and simulation of carrier heating with effects of nonequilibrium hot phonons in semiconductor photovoltaic devices," Prog. Photovoltaics Res. Appl. **26**(10), 808–824 (2018).

[12]Y. Zhang, L. Tang, B. Zhang, P. Wang, and C. Xu, "Quantitative study on the mechanisms underlying the phonon bottleneck effect in InN/InGaN multiple quantum wells," Appl. Phys. Lett. **116**(10), 103104 (2020).

[13]J.A. Dimmock, S. Day, M. Kauer, K. Smith, J. Heffernan, "Demonstration of a hot-carrier photovoltaic cell", Progress in Photovoltaics: Research and Applications, 22(2), 151-160 (2014).

[14]J.A. Dimmock, M. Kauer, J. Wu, H. Liu, P.N. Stavrinou, N.J. Ekins-Daukes, "A metallic hot-carrier photovoltaic device", Semiconductor Science and Technology, 34(6), 064001 (2019).

[15]N. Cavassilas, F. Michelini, M. Bescond, T. Joie, "Hot-carrier solar cell NEGF-based simulations," Physics, Simulation, and Photonic Engineering of Photovoltaic Devices V, 97430R (2016).

[16]I. Massiot, A. Cattoni, and S. Collin, "Progress and prospects for ultrathin solar cells," Nat. Energy **5**, 959-972 (2020).

[17]N Cavassilas, F Michelini, M Bescond, "Modeling of nanoscale solar cells: The Green's function formalism," J. of Renewable and Sustainable Energy **6**(1), 011203 (2014).

[18]A Yangui, M Bescond, T Yan, N Nagai, K Hirakawa, "Evaporative electron cooling in asymmetric double barrier semiconductor heterostructures," Nature communications **10**(1), 1-7 (2019).

[19]J. Fast, U. Aeberhard, S. Bremner, H. Linke, “Hot-carrier optoelectronic devices based on semiconductor nanowires,” Applied Physics Reviews **8**(2), 021309 (2021).

[20]H. Esmaielpour, L. Lombez, M. Giteau, A. Delamarre, D. Ory, A. Cattoni, S. Collin, J.-F. Guillemoles, D. Suchet, “Investigation of the spatial distribution of hot carriers in quantum-well structures via hyperspectral luminescence imaging,” J. Appl. Phys. **128**(16), 165704 (2020).

[21]B. Galvani, D. Suchet, A. Delamarre, M. Bescond, F. Velia Michelini, M. Lannoo, J.-F. Guillemoles, N. Cavassilas, “Impact of Electron–Phonon Scattering on Optical Properties of $CH_3NH_3PbI_3$ Hybrid Perovskite Material,” ACS omega 4 (25), 21487-21493 (2019).

[22]A. P. Kirk and M. V. Fischetti, “Fundamental limitations of hot-carrier solar cells,” Phys. Rev. B **86**(16), 165206 (2012).

[23]S. Limpert, A. Burke, I-J. Chen, N. Anttu, S. Lehmann, S. Fahlvik, S. Bremner, G. Conibeer, C. Thelander, M.-E. Pistol, “Single-nanowire, low-bandgap hot carrier solar cells with tunable open-circuit voltage,” Nanotechnology **28**(43), 434001 (2017).

[24]F. Michelini, A. Crépieux, K. Beltako, “Entropy production in photovoltaic-thermoelectric nanodevices from the non-equilibrium Green’s function formalism,” J. Phys.: Cond. Mat. 29, 175301 (2017).

[25]M.F. O’Dwyer, T.E. Humphrey, R.A. Lewis, C. Zhang, “Electronic and thermal transport in hot carrier solar cells with low-dimensional contacts,” Microelectronics Journal, 39(3-4), 656-659 (2008).